

## Preparation of astaxanthin/zeaxanthin-loaded nanostructured lipid carriers for enhanced bioavailability: Characterization-, stability- and permeability study

### ABSTRACT

KRISTINA RADIC<sup>1</sup>   
ANA ISABEL BARBOSA<sup>2</sup>   
SALETTE REIS<sup>2</sup>   
MARIJAN MARIJAN<sup>3</sup>   
SOFIA ANTUNES COSTA LIMA<sup>4\*</sup>   
DUBRAVKA VITALI ČEPO<sup>\*</sup> 

<sup>1</sup> University of Zagreb  
Faculty of Pharmacy and Biochemistry  
Department of Food Chemistry  
10000 Zagreb, Croatia

<sup>2</sup> LAQV, REQUIMTE, Departamento  
de Ciências Químicas, University of  
Porto, 4050-313 Porto, Portugal

<sup>3</sup> University of Zagreb  
Faculty of Pharmacy and Biochemistry  
Department of Pharmacognosy  
10000 Zagreb Croatia

<sup>4</sup> LAQV, REQUIMTE, Instituto de  
Ciências Biomédicas de Abel Salazar  
University of Porto, 4050-313 Porto  
Portugal

Astaxanthin (ASTA) and zeaxanthin (ZEA) are xanthophyll carotenoids showing a wide spectrum of health-promoting properties. However, their utilization is limited, mostly due to poor water solubility, limited bioavailability, and a tendency to oxidate, as well as photo- and thermal instability. The aim of this work was to develop ASTA- and ZEA-loaded nanostructured lipid carriers (NLCs) that would protect them against degradation and improve their intestinal stability/permeability. Obtained NLCs were characterized by an effective diameter of 294 nm for ASTA-NLC and 280 nm for ZEA-NLC; polydispersity index (*PDI*) lower than 0.2; and zeta potential of  $-29.4$  mV and  $-29.0$  mV, respectively. Interestingly, despite similar physicochemical characteristics, our investigation revealed differences in the encapsulation efficiency of ASTA-NLC and ZEA-NLC (58.0 % vs. 75.5 %, respectively). Obtained NLCs were stable during a 21 day-storage period in the dark at room temperature or at 4 °C. Investigation of gastrointestinal stability showed no change in effective diameter and *PDI* under gastric conditions while both parameters significantly changed under intestinal conditions. Our results showed for the first time that both ASTA- and ZEA-NLCs intestinal absorption investigated in the *in vitro* model is significantly increased (in relation to pure compounds) and is affected by the presence of mucus. This study provides useful data about the advantages of using NLC as a delivery system for ASTA and ZEA that might facilitate their applications in the food and pharmaceutical industry.

**Keywords:** gastrointestinal stability, nutraceuticals, poor water solubility compounds, xanthophylls

Accepted June 12, 2023  
Published online September 7, 2023

Carotenoids and their oxygenated derivatives xanthophylls are among the most important natural pigments because of their wide distribution in plant tissues, structural diversity, and numerous functions in the human body. A series of studies have demonstrated that

\*Correspondence; e-mails: dubravka.vitali@pharma.unizg.hr; slima@icbas.up.pt

xanthophylls act as health promoters, specifically, in the prevention and treatment of cardiovascular, gastrointestinal (GI), hepatic, neurodegenerative, ocular, and dermatological diseases, as well as diabetes, diabetic neuropathy, metabolic syndromes, cancer, and chronic inflammation (1).

Astaxanthin (ASTA, 3,3'-dihydroxy- $\beta,\beta$ -carotene-4,4'-dione), a lipid-soluble pigment belonging to the xanthophyll class of carotenoids (Fig. 1a), is mainly obtained from algae, yeast, trout, red seabream, and waste of crustaceans such as shrimp and crabs (2). There is tremendous interest in ASTA due to its functional characteristics, both in the food industry, because of its bright red color, but also in the pharmaceutical industry. Namely, ASTA has been characterized by strong antioxidant activity and a range of health benefits such as anticancer, neuroprotective, immunomodulatory, and cardioprotective effects (3).

Zeaxanthin (ZEA, (3*R*,3'*R*)- $\beta,\beta$ -carotene-3,3'-diol) is a lipid-soluble pigment belonging to the xanthophyll class of carotenoids (Fig. 1b) which is found in dark green vegetables, orange and yellow fruits, and egg yolks. It exhibits strong antioxidative activity, particularly in the eye region, since ZEA accumulates in the macula. Many studies prove that a diet rich in ZEA prevents the progression of eye diseases such as cataracts and age-related macular degeneration which can lead to blindness. The knowledge about other desirable effects of ZEA on human health, such as anticancer, cardioprotective, antidiabetic, and neuroprotective effects, is increasing (4).

It is evident that the use of ASTA and ZEA as functional food ingredients or nutraceuticals has practical significance for improving human health and well-being (5). However, their utilization in the food and pharmaceutical industry faces many challenges mainly due to poor water solubility, susceptibility to oxidation, and photo- and thermal instability. The poor water solubility of ASTA and ZEA presents a major obstacle to their satisfactory oral bioavailability (since it is directly dependent on their dispersibility in the water medium). Moreover, the instability of ASTA and ZEA leads to significant losses that occur during processing, storage, and GI digestion with negative impacts on bioavailability and, consequently, bioactivity (6). Therefore, it is evident that the efficient incorporation of ASTA/ZEA into functional food or nutraceuticals must be preceded by an advanced

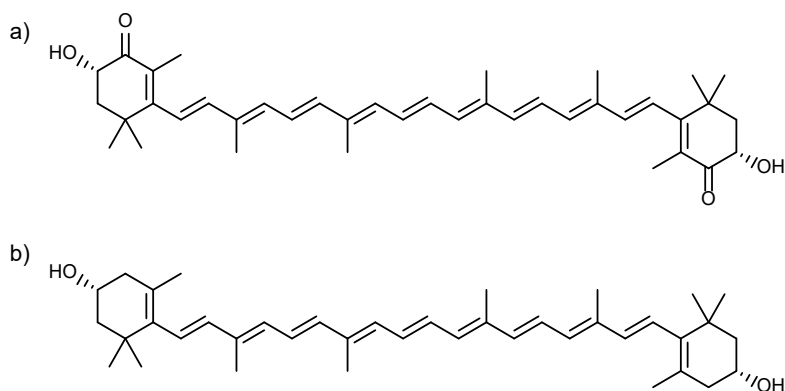


Fig. 1. Structures of: a) astaxanthin and b) zeaxanthin.

formulation that would provide protection against degradation and improved solubility/bioavailability (5).

In recent years, a significant amount of research has been devoted to investigating the applicability of various delivery systems that would improve carotenoid properties. Several types that have already been used to improve the functionality of liposoluble bioactive compounds can generally be classified as lipid-based delivery systems and polymer-based delivery systems. In particular, lipid-based nano-delivery systems (such as nanoemulsions, liposomes, solid lipid nanoparticles, and nanostructured lipid carriers (NLCs) have been shown to improve the stability and bioavailability of certain carotenoid classes. However, the majority of research has been devoted to the encapsulation of ASTA in liposomes (7) and solid lipid nanoparticles (8) while the possibilities of encapsulation in NLC of ASTA and especially ZEA have not been thoroughly investigated.

Considering all the above, the formulation of innovative delivery systems for ASTA and ZEA to improve their solubility, stability, bioavailability, and consequently, health efficacy, is highly desired.

NLCs are an innovative delivery system for encapsulation of bioactive compounds characterized by poor water solubility which has been proven to increase their stability and bioavailability. Even though NLCs may dispel some of the disadvantages of other lipid nanocarriers, such as low encapsulation efficiency (*EE*), low drug loading, and physico-chemical instability, they also have benefits that make them suitable for a wide range of applications (9, 10). They usually have higher loading capacity than other lipid nanocarriers and raw materials for their production can be selected from low-cost-, food-grade-, and generally recognized as safe (GRAS) materials. In the food industry, NLCs have been shown to be suitable for encapsulating and incorporating lipophilic compounds (bioactives, flavors, and antimicrobials) into water-based foods. The utilization of NLCs as drug delivery systems has been explored for many compounds and resulted in their improved stability and bioavailability. It has been shown that NLC-based nanosystems can be used to enable controlled release of the active ingredients, both sustained and delayed releases, which are time- or site-dependent. Thus, NLCs may be utilized as efficient delivery systems, for food and pharmaceutical industries.

Based on all of the above, it can be assumed that NLCs might present a suitable formulation approach for improving the storage- and GI stability of ASTA and ZEA and for enhancing their permeability. The presence of lipids in delivery systems of ASTA has already been proven to increase its permeability in Caco-2 cells (where ASTA was encapsulated in nanoemulsions (11, 12) and liposomes (13, 14). The same has been presented for several highly lipophilic molecules such as curcumin (15, 16) and lutein (17). Also, the conclusions from a small number of *in vivo* studies strongly suggest that the bioavailability of ASTA can be significantly improved when taken with meal/lipids (18, 19). Little is known about potentially beneficial effects of incorporating ZEA within lipid-based delivery systems. However, ZEA faces the same stability/permeability issues as other carotenoids; therefore, it can be assumed that certain improvements can be also achieved through its incorporation into lipid-based delivery systems. The permeability of ASTA/ZEA, the fraction that passes through the mucus layer across the epithelium cells and into the systemic circulation, is the limiting step to their satisfactory bioavailability. In order to evaluate the applicability of the newly designed delivery system for incorporation of ASTA/ZEA, it is, therefore, advisable to perform a digestive stability/permeability study. For this purpose,

*in vitro* static models are widely used since they are easy to build and require lower amounts of samples. Significant improvements in mimicking digestion and intestinal absorption *in vitro* have been achieved but still little is understood on mucus interference with both specific molecules and with the delivery system within it is incorporated. The matter is still unclear, so it presents a hot topic of many scientific discussions. Some authors concluded that the mucus presence relates to the lower recovery of hydrophobic bioactive compounds while others demonstrated that lipid-based delivery systems may improve their permeability through the mucus barrier of hydrophobic moieties. Namely, Li and coworkers reported that the mucus layer covering cell co-cultures was associated with the lower recoveries of both hydrophilic epigallocatechin-3-gallate and hydrophobic  $\beta$ -carotene (20). On the other hand, Cai and coworkers recently reported that hydrophobic cinnamaldehyde in self-emulsifying drug delivery systems (SEDDS) exhibited good release and superior mucus permeability (21).

The aim of this work was to improve the functional properties of ASTA and ZEA by incorporating them into novel lipid-based formulations, primarily targeting their solubility, storage- and GI- stability, and intestinal permeability. For that purpose, innovative NLCs were formulated by organic solvent-free hot homogenization procedure using an ultrasonicator. Obtained NLCs were characterized, and their physicochemical properties, as well as their storage- and GI stabilities were reported. Moreover, the impact of mucus on the permeability of free-, and ASTA- and ZEA-incorporated NLC was studied. The results of this study will provide useful data that will contribute to the efforts for successful incorporation of liposoluble bioactive compounds into NLCs and encourage their utilization as delivery systems for potential applications in the food and pharmaceutical industry.

## EXPERIMENTAL

### Materials

ASTA and ZEA standards were obtained from Biosynth (UK). Precirol<sup>®</sup> ATO5 was kindly provided by Gattefossé (France). Miglyol<sup>®</sup> 812 was obtained from Acofarma<sup>®</sup> (Spain). Fasted-state simulated gastric fluid (FaSSGF) and fasted-state simulated intestinal fluid (FaSSIF) were obtained from Biorelevant (UK). FaSSGF solution was characterized with pH 1.6 and composed of 0.08 mmol L<sup>-1</sup> taurocholate, 0.02 phospholipids, 34 mmol L<sup>-1</sup> sodium, and 59 mmol L<sup>-1</sup> chloride while FASSIF was characterized with pH 6.5 and composed of 3 mol L<sup>-1</sup> taurocholate, 0.75 phospholipids, 148 mmol L<sup>-1</sup> sodium, 106 mmol L<sup>-1</sup> chloride, and 29 mmol L<sup>-1</sup> phosphate. Caco-2 and HT29 cells were obtained from ATCC-LGC Standards (Spain). Dulbecco's modified eagle's medium (DMEM), penicillin-streptomycin, fetal bovine serum (FBS), and amphotericin B were purchased from Gibco<sup>®</sup> Invitrogen Corporation (USA). Nonessential amino acids (NEAA), trypsin, Triton X-100, phosphate buffer saline (PBS), Hanks' balanced salt solution (HBSS), acetonitrile, Trolox, Tween<sup>®</sup> 80 (polysorbate 80), dimethyl sulfoxide (DMSO), and 3-(4,5-dimethylthiazol-2-yl)-2,5-diphenyltetrazolium bromide (MTT) were acquired from Sigma-Aldrich (USA). All water used was double-deionized water collected from the Sartorius AG Arium Pro apparatus (Germany).

### *Preparation of NLCs loaded with ASTA and ZEA*

The nanoparticles were prepared by an organic solvent-free hot homogenization procedure using an ultrasonicator (22). The optimal composition of the NLC was obtained with the following procedure (presented in Table I): 2 mg of ASTA or ZEA, 1 mg of Trolox, 50 mg of Miglyol® 812, 250 mg of Precirol® ATO5, and 80 mg of Tween® 80 were mixed and heated in a water bath at 72 °C for 30 min followed by additional heating at 90 °C for 5 min. 6 mL of degassed ultrapure water heated at 90 °C was added and the sample was homogenized with a probe-type sonicator VCX-130 with a VC 18 probe by Sonics & Materials Inc (USA) for 5 min at the amplitude of 70 % to form the nanoparticle suspension. Immediately after ultrasonication, the samples were put on ice for 10 min and stored in glass tubes, purged with argon, and protected from light.

*Table I. Composition of the reaction mixture for NLC preparation*

| Component                | Amount  |
|--------------------------|---------|
| ASTA or ZEA              | 2 mg    |
| Trolox                   | 1 mg    |
| Miglyol® 812             | 50 mg   |
| Precirol® ATO5           | 250 mg  |
| Tween® 80                | 80 mg   |
| Ultra-pure water (90 °C) | 6 mL    |
| ASTA/ZEA : lipid         | 1 : 150 |

### *Determination of encapsulation efficiency and drug loading*

The incorporation of ASTA/ZEA into the NLCs was assayed through a direct pressure ultrafiltration method with Amicon®. The NLCs were separated from the suspension (which may contain non-incorporated ASTA/ZEA) and destroyed with acetonitrile. Briefly, the formulations were diluted 40 times in double deionized water and 2 mL of this dilution were filtrated with EMD Millipore Amicon® Ultra Centrifugal Filters Ultracell-50 kDa (Germany), at 3500 ×g for 45 min, using a Thermo Fisher Scientific Heraeus Multifuge X1R centrifuge (USA). The supernatant was discarded and the pellet present in the filtrate unit was recovered through centrifugation at 4500 ×g for 15 min. Then, the pellet was resuspended in 1950 µL of acetonitrile to destabilize the particles and to release the entrapped analyte. The mixture was then transferred to a 2 mL Eppendorf tube and centrifugated for 30 min at 10000 ×g to separate the lipids and the supernatant was used for absorbance (A) read-out. To prevent reaching A values out of the calibration range, the final solution was diluted with acetonitrile.

All A readings were obtained at 450 nm with Agilent BioTek Synergy HTX Multimode Reader (USA). A calibration curve of UV/Vis detection of ASTA/ZEA with a range of 0.9–30 µg mL<sup>-1</sup>, was performed for further use in ASTA/ZEA incorporation assays. The coefficients of correlation for both analytes were 0.999.

The encapsulation efficiency (*EE*) was calculated according to *Equation 1*, defined as the quotient between the determined mass of ASTA/ZEA in the NLCs retained within the Amicon® filter and the total amount of initially added ASTA/ZEA in the NLCs preparation.

$$EE(\%) = \frac{m_{\text{exper ASTA/ZEA}}}{m_{\text{init ASTA/ZEA}}} \times 100 \quad (1)$$

The drug loading (*DL*) was calculated according to *Equation 2*, defined as the quotient between the incorporated mass of ASTA/ZEA in the NLCs and the mass of NLCs .

$$DL(\%) = \frac{m_{\text{incorp ASTA/ZEA}}}{m_{\text{NLC}}} \times 100 \quad (2)$$

### *Determination of particle size and zeta potential*

The mean effective diameter and polydispersity index (*PDI*) for NLCs were determined through dynamic light scattering (DLS) using a Brookhaven Instruments Corporation 90 Plus Particle Size Analyzer (USA). Zeta potential was determined using a Brookhaven Instruments Corporation Zeta Potential Analyzer. For both DLS and zeta potential analysis, the formulations were diluted 200 times in double deionized water and all readings were performed with six runs each. The instrument is equipped with a 35-mW solid-state red laser (660 nm wavelength), operating at a scattering angle of 90°, and acquiring the measurements at 20 °C. The obtained size was determined from the intensity of scattered light, and the count rate values obtained for 1:200 diluted samples were within the recommended range for the equipment following Brookhaven Instruments instructions (300–500 kcps – counts per second). The refractive index for the NLCs was 1.33. Each different batch of NLCs was individually characterized, having the mean size ± SD calculated after 6 runs of 2 minutes each (12 minutes of analysis per sample). The surface charge of NLCs (Zeta potential) was possible to determine using an electrode also operating at a scattering angle of 90° at 20 °C. For each different batch of NLCs assay, the mean zeta potential ± SD is calculated as the average of 6 runs of 10 cycles. Whenever in need of nanoparticle suspension measurements, the parameters of the DLS software were adjusted to the ones of double deionized water at 20 °C: dynamic viscosity of 1.002 cP and a pH value of cca 6–7. Double-deionized water contains a minimum amount of ions and thus has a low buffering capacity. Therefore, for each measurement of NCL suspension, freshly collected double-deionized water, provided by an ultra-pure water system was used (AriumPro, Sartorius AG, Germany).

### *Determination of storage stability*

For investigation of stability during storage, samples were transferred into a brown glass volumetric flask immediately after the preparation. They were then flushed with argon and stored in the dark at room temperature and at 4 °C. Storage stability studies were conducted by measuring the variations of effective diameter, *PDI*, and zeta potential during the storage period of 21 days.

### Determination of GI stability

The stability of ASTA/ZEA NLCs was assessed by *in vitro* static simulation of GI digestion in the upper tract by using biorelevant media. Briefly, 100 µL of the NLC formulations were added to 19900 µL of a FaSSGF or FaSSIF or water (23). The mixtures were kept simultaneously at 37 °C in a thermostatic shaker for 2 hours with constant stirring at 110 rpm after which the effective diameter and *PDI* were determined.

### Permeability study

#### Cell cultures

For investigation of permeability, human epithelial colorectal adenocarcinoma cell lines, Caco-2 and HT29 were used. Caco-2 cells (American Type Culture Collection (ATCC)) were cultured in complete DMEM supplemented with 10 % (V/V) heat-inactivated FBS, 1 % (V/V) NEAA, and 1 % (V/V) penicillin/ streptomycin/amphotericin B mixture. HT29 cells (ATCC) were cultured in McCoy's 5a Medium Modified supplemented with 10 % (V/V) heat-inactivated FBS, 1 % (V/V) NEAA, and 1 % (V/V) penicillin/streptomycin/amphotericin B mixture. Cell cultures were maintained at 37 °C, in a humidity-saturated atmosphere consisting of 5 % CO<sub>2</sub> in Sanyo MCO-20AIC CO<sub>2</sub> Incubator (Osaka, Japan). The medium was replaced by fresh, complete media every three days. Cells were passaged by trypsinization at 80–90 % confluence.

### Evaluation of biocompatibility by MTT assay

When cells were confluent, they were detached from the culture flask by trypsinization. Briefly, the media was removed and washed with 5 mL of fresh media without FBS. Then the cells were incubated at 37 °C with 5 mL of trypsin. Trypsinization was stopped by adding fresh media with FBS. After the detachment, cells were homogenized, transferred to 50 mL Falcon tubes, and centrifuged at 300 ×g for 5 min in a Thermo Fisher Scientific Heraeus Multifuge X1R centrifuge. Then the cells were resuspended in fresh complete media and cultivated in a transparent 96-well plate at a density of 5 × 10<sup>4</sup> cells per well, in 100 µL of fresh culture media. Once the cells had adhered, the medium was replaced with complete media containing different concentrations of pure ASTA/ZEA or NLCs (loaded with ASTA/ZEA). Cells were treated with either pure ASTA in concentrations of 20–100 µg mL<sup>-1</sup>; pure ZEA in concentrations of 10–50 µg mL<sup>-1</sup>; NLC loaded with ASTA in concentrations of 2–6 mg mL<sup>-1</sup> (in which ASTA is in concentrations of 0.4–1.1 µg mL<sup>-1</sup>); and NLC loaded with ZEA in concentrations of 1–5 mg mL<sup>-1</sup> (in which ZEA is in concentrations of 0.2–1.2 µg mL<sup>-1</sup>) for 24-hours. Control cells were also included in every plate (negative control (ctr-) contained only complete media while positive control (ctr+) was treated with Triton X-100). The cells were incubated for 24 h under the same conditions as described above and afterwards, the medium was replaced by 100 µL of a 0.5 mg mL<sup>-1</sup> MTT solution diluted in complete media. The plates were incubated for 3 h at 37 °C, after which the MTT solution was aspirated and 100 µL of DMSO was added to solubilize the formazan crystals. The absorbance was read at 570 and 630 nm using Agilent BioTek Synergy HTX Multimode Reader. Cell viability was defined as described in Equation 3.

$$\text{Cell viability (\%)} = \frac{(A_{570} - A_{630})_{\text{ASTA/ZEA}}}{(A_{570} - A_{630})_{\text{ctr}}} \times 100 \quad (3)$$

### Permeability study

Permeability study was conducted in a 12-well plate with Costar 3401, Corning Incorporated Transwell® permeable supports (USA) (24).  $3 \times 10^4$  Caco-2 cells were seeded alone or with the addition of  $7 \times 10^3$  HT29 cells in each Transwell® and kept at 37 °C, in a humid saturated atmosphere consisting of 5 % CO<sub>2</sub>. Cells were grown for 23 days to form a differentiated monolayer. The medium was aspirated and replaced every 2 days. The added volume was 0.5 mL in the apical and 1.5 mL in the basolateral compartment. Monolayer integrity was routinely checked by determining transepithelial electrical resistance (TEER) during the cell growth, before and after the transport experiment. ER was measured with World Precision Instruments Inc STX2 and EVOM resistance meter (USA).

To determine transepithelial permeability, the medium was aspirated from both apical and basolateral chambers and washed with pre-warmed PBS. Then, 0.5 mL of the samples were added to the apical chamber and 1.5 mL of the HBSS with 4 % of FBS to the basolateral chamber of each well (25). FBS was added to the recipient in order to improve the solubility of ASTA/ZEA in a buffer. Samples were applied on a cell monolayer in triplicates and incubated at 100 rpm and 37 °C for 2 h in a Biosan Incubator ES-20/60 (Latvia). The content of ASTA/ZEA was determined by measuring absorbance (as described previously) in an apical chamber and expressed as % of the amount applied on the cell monolayer (calculated according to Equation 4).

$$\text{Intestinal absorption (\%)} = \frac{\text{amount in apical compartment}}{\text{initial amount}} \times 100 \quad (4)$$

### Statistical analysis

Obtained results were expressed as average values and standard deviations from a minimum of three independent experiments. Data were statistically evaluated by either Student *t*-test to compare two groups of independent samples, or by one-way analysis of variance (ANOVA) to compare multiple groups of independent samples. For that purpose, GraphPad®Prism 6 Software (USA) was used. When the groups presented a significant statistical difference ( $p \leq 0.05$ ), the differences between the respective groups were compared with a post-hoc Tukey test.  $p \leq 0.05$  was considered statistically significant unless otherwise noted.

## RESULTS AND DISCUSSION

Newly synthesized ASTA-NLC and ZEA-NLC were composed of a mixture of solid and liquid lipids (Precirol® ATO 5 and Miglyol® 812, respectively) and a surfactant (Tween® 80) forming an unstructured solid matrix in an aqueous solution. NLC preparation was conducted by the hot homogenization method previously described (22). After the complete addition of aqueous solution over the oil phase, the obtained formulations were cooled down at room temperature. NLC suspensions were characterized by effective diameter, *PDI*, zeta potential, *EE*, and *DL*.

### Physicochemical characterization of nanoparticles

Obtained results revealed that ASTA-NLC, ZEA-NLC as well as empty NLC (B-NLC) had similar physicochemical characteristics showing no statistically significant difference in effective diameter, *PDI*, and zeta potential. The average effective diameter was 294 nm for ASTA-NLC, 280 nm for ZEA-NLC, and 267 nm for B-NLC. *PDI* was in the range of 0.137–0.152 and zeta potential was from –28.8 to –29.4 mV (Table II). There was a statistically significant difference in *EE* of ASTA and ZEA ( $58.0 \pm 6.9\%$  and  $75.5 \pm 2.3\%$ , respectively).

Table II. Physicochemical characteristics of obtained NLCs<sup>a</sup>

| Parameter               | ASTA-NLC      | ZEA-NLC       | B-NLC         |
|-------------------------|---------------|---------------|---------------|
| Effective diameter (nm) | 293.8 ± 9.7   | 280.2 ± 14.5  | 268.8 ± 31.0  |
| <i>PDI</i>              | 0.152 ± 0.014 | 0.141 ± 0.023 | 0.137 ± 0.003 |
| Zeta potential (mV)     | –29.39 ± 0.91 | –29.00 ± 0.37 | –28.81 ± 3.50 |
| <i>EE</i> (%)           | 58.0 ± 6.9    | 75.5 ± 2.3*   |               |
| <i>DL</i> (%)           | 0.39 ± 0.05   | 0.50 ± 0.02*  |               |

<sup>a</sup> *EE* was calculated according to Equation 1. *DL* was calculated according to Equation 2. \* indicates the significant difference of *EE* among samples ( $p < 0.02$ ).

### Stability assays

Stability studies of NLC, both stored at room temperature in the dark and at 4 °C in the dark were conducted by measuring the variations of effective diameter, *PDI*, and zeta potential during the storage period of 21 days.

According to Fig. 2, all NLC samples seem to be stable over 21 days since their effective diameter (Fig. 2a) and polydispersity (Fig. 2b) were not significantly changed in relation to freshly prepared formulations. Zeta potential values of samples also remained constant (Fig. 2c).

ASTA- and ZEA-NLCs stability in the GI tract was assessed by *in vitro* static simulation of GI digestion in the upper tract by using biorelevant (FaSSGF and FaSSIF) media in terms of effective diameter and *PDI*. The result showed that both ASTA-NLC and ZEA-NLC did not change effective diameter and *PDI* under gastric conditions (Fig. 3). On the other hand, statistically significant increase of both effective diameter and *PDI* of ASTA-NLC and ZEA-NLC was observed under intestinal conditions (Fig. 3). More precisely, the effective diameter of ASTA-NLC increased from 271 nm in water to 332 nm in FaSSIF while effective diameter of ZEA-NLC increased from 257 nm in water to 363 nm in FaSSIF. The *PDI* also significantly increased in FaSSIF for both samples when compared to the sample in water. More precisely, the *PDI* of ASTA-NLC increased from 0.128 in water to 0.262 in FaSSIF whereas the *PDI* of ZEA-NLC increased from 0.122 in water to 0.264 in FaSSIF.

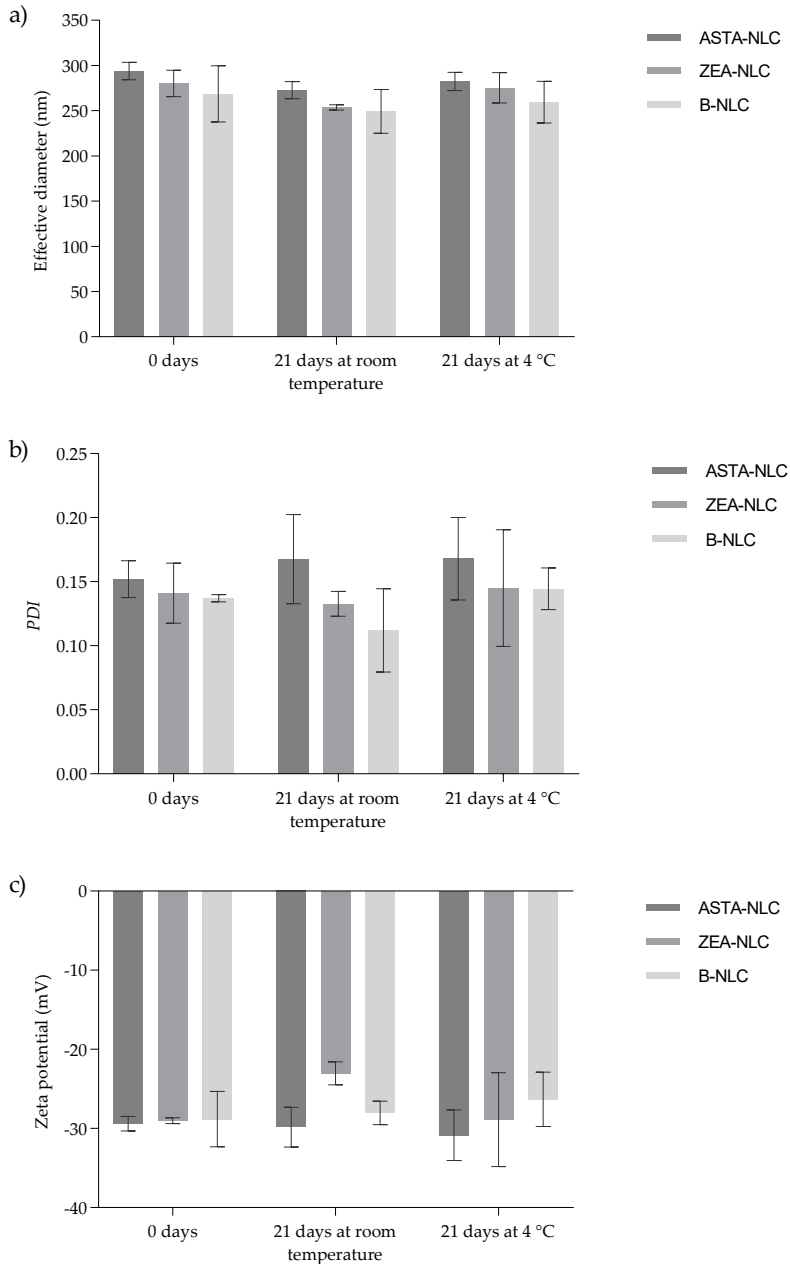


Fig. 2. Storage stability of ASTA-NLC, ZEA-NLC and B-NLC over the period of 21 days at room temperature or at 4 °C in the dark. The observed parameters were: a) effective diameter, b) *PDI*, and c) zeta potential. Data are presented as mean ± standard deviation ( $n = 3$ ).

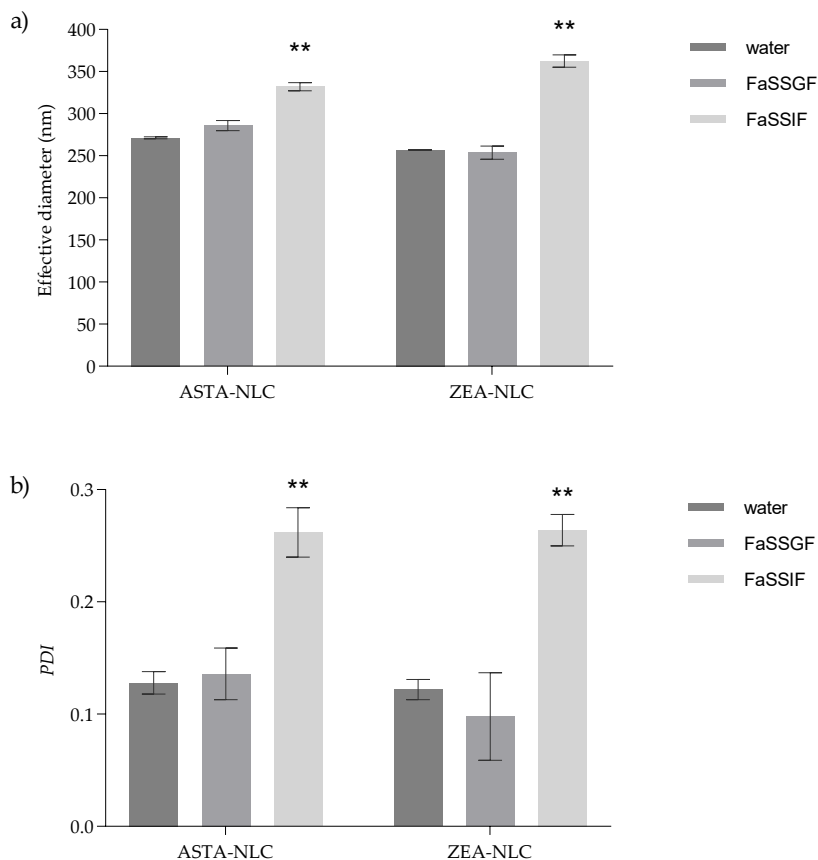


Fig. 3. GI stability of ASTA-NLC and ZEA-NLC. The observed parameters were: a) effective diameter and b) *PDI*. Data are presented as mean  $\pm$  standard deviation ( $n = 3$ ). \*indicate the significant difference of results for every sample ( $p < 0.001$ ).

### *Biocompatibility*

The influence of ASTA, ZEA, ASTA-NLC, or ZEA-NLC on the viability of human epithelial colorectal adenocarcinoma cells (Caco-2) was determined by the MTT assay. The results presented in Fig. 4 showed a proportional decrease in cell viability with increasing concentration of analyzed samples. The purpose of the biocompatibility study was to determine the concentration of the sample that enables at least 80 % cell viability (marked with a horizontal line in Fig. 4a-d). Obtained results showed that exposure to both ASTA and ZEA in a concentration of  $20 \mu\text{g mL}^{-1}$  enables at least 80 % cell viability of Caco-2 cells while exposure to both ASTA-NLC and ZEA-NLC enables at least 80 % cell viability of Caco-2 cells in a concentration of  $3 \text{ mg mL}^{-1}$  (in which ASTA or ZEA are in a concentration of  $0.6 \mu\text{g mL}^{-1}$ ).

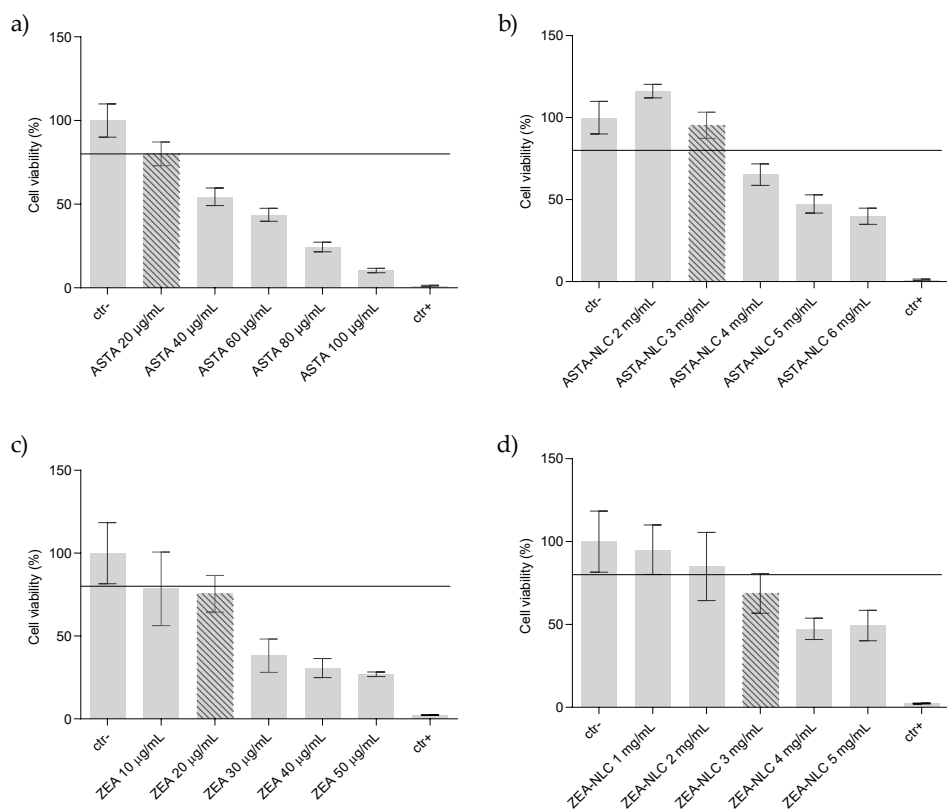


Fig. 4. Effect of a 24-hour exposure of: a) ASTA, b) ASTA-NLC, c) ZEA, and d) ZEA-NLC on Caco-2 cell viability. Data are presented as mean  $\pm$  standard deviation of cell viability percentage calculated according to Equation 3. All experiments were done in triplicate. The horizontal line represents 80 % cell viability.

### Permeability study

A permeability study was conducted in order to investigate the impact of the incorporation of ASTA and ZEA into NLCs on intestinal transepithelial permeability. Additionally, the relevance of mucus for the ASTA and ZEA permeability was investigated by comparing permeability data obtained in Caco-2 and Caco-2/HT29 cell models, respectively.

The content of ASTA/ZEA was determined in the apical chamber and expressed as a percent of the amount applied on the cell monolayer according to Equation 4. The results presented in Fig. 5 showed that both ASTA and ZEA intestinal absorption was significantly increased in the form of NLC, regardless of the presence of mucus. Namely, ASTA intestinal absorption increased from 7.5 % to 20.3 % on the Caco-2 cell model ( $p < 0.0001$ ) and from 8.3 % to 27.7 % on the Caco-2/HT29 cell model ( $p < 0.0001$ ). ZEA intestinal absorption increased from 7.1 % to 17.7 % on the Caco-2 cell model ( $p < 0.0001$ ) and from 9.8 % to

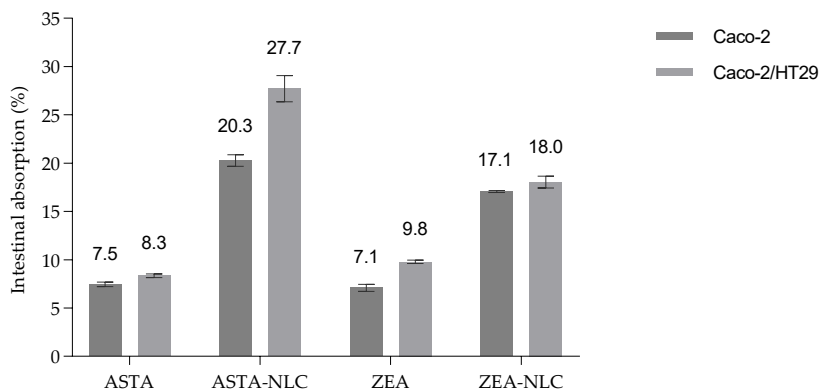


Fig. 5. Permeability of ASTA, ASTA-NLC, ZEA, and ZEA-NLC in Caco-2 and Caco-2/HT29 cell models. Data represents the absorbed fraction of analytes calculated according to Equation 4 and expressed as the percentage of the initial amount applied on the cell monolayer. All experiments were conducted in triplicate ( $n = 3$ ).

18.8 % on the Caco-2/HT29 cell model ( $p < 0.0001$ ). Overall, the intestinal absorption of ASTA-NLC increased by 3-fold in respect to free form while the intestinal absorption of ZEA increased by 2-fold in respect to free form.

By comparing results obtained in the Caco-2- and Caco-2/HT29 cell model it was observed that the presence of mucus had a positive impact on the intestinal absorption for both analytes applied in free form, while the effect was mixed for investigated NLCs. Namely, in the presence of mucus, the intestinal absorption of ASTA in the free form increased from 7.5 % to 8.3 % ( $p = 0.0249$ ) while the intestinal absorption of ZEA in the free form increased from 7.1 % to 9.8 % ( $p < 0.0001$ ). The presence of mucus also increased the intestinal absorption of ASTA-NLC since the permeability increased from 20.3 to 27.7 % ( $p < 0.0001$ ) while it did not have an impact on the intestinal absorption of ZEA-NLC (Fig. 5). Moreover, there was no difference in intestinal absorption of ASTA and ZEA in Caco-2 cell model while on Caco-2/HT29 cell model, ZEA intestinal absorption was significantly higher compared to ASTA ( $p = 0.0005$ ). On the other hand, ASTA-NLC intestinal absorption was significantly higher than ZEA-NLC in both, the Caco-2 ( $p = 0.0044$ ) and Caco-2/HT29 ( $p < 0.0001$ ) cell models.

## Discussion

Newly designed ASTA-NLC and ZEA-NLC were composed of a mixture of solid and liquid lipids (Precirol® ATO 5 and Miglyol® 812, respectively) and a surfactant (Tween® 80) forming an unstructured solid matrix in aqueous solution. Obtained results revealed that ASTA-NLC, ZEA-NLC, and B-NLC had comparable physicochemical characteristics regarding effective diameter, *PDI*, and zeta potential.

The mean particle size and the particle size distribution (usually *PDI*) are the most important characteristics of NLCs that govern the physical stability, solubility, biological

performance, release rate, turbidity, and chemical stability. Based on pharmaceutical literature, the NLC average diameter is usually in the range of 50–1000 nm (26). In this study, the effective diameter was 294 nm for ASTA-NLC, 280 nm for ZEA-NLC, and 267 nm for B-NLC indicating that particles will be able to penetrate through biomembranes. Namely, particles with sizes less than 400 nm are characterized by improved permeability which is an important prerequisite for adequate oral bioavailability of ASTA and ZEA since it is known that the permeability is intrinsically low for this type of lipophilic micro-nutrients (27, 28). Available studies on ASTA and ZEA incorporated into NLCs are scarce but promising. In the present case, the ASTA-NLC exhibited higher effective diameter compared to those reported by Tamjidi and coworkers (29) and Rodriguez-Ruiz and coworkers (30) (which were 94 nm and 60 nm, respectively), and similar to the one reported by Huang and coworkers (31) which was around 200 nm. According to our knowledge, there is just one group that recently incorporated ZEA into NLCs and obtained ZEA-NLC characterized with a smaller average effective diameter which did not exceed 130 nm (32).

The *PDI* reflects the range of primary sizes of nanoparticles in the suspension and influences their tendency to aggregate (33); therefore it should be as low as possible in order to ensure the long-term stability of NLC. Here the obtained *PDI* values were in the range of 0.137–0.152 (Table II), which is significantly lower in comparison to those previously reported in the literature (29, 30, 34). Low polydispersity values indicate homogeneity and monodispersity of NLC formulations. Observed differences in effective diameter and *PDI* values, compared to literature data, are the result of the nature and the content of the blend of lipids/surfactant employed in the formulation process (35).

The zeta potential is the electrical potential at the shear plane, which is defined as the distance from the particle surface below which the counter-ions remain strongly attached to the particle when it moves in an electrical field (36). It is an indirect measure of the physical stability of NLC, and it can influence the kinetic and biological fate of nanoparticles. For nanosuspensions that are stabilized by combined electrostatic and steric forces, a minimum zeta potential of  $\pm 20$  mV is desirable (37). If all particles in the suspension have a high negative or positive zeta potential then there will be no tendency for the particles to aggregate because they will repel each other (38). According to zeta potential measurements presented in Table II (ranging from  $-28.8$  to  $-29.4$  mV), both ASTA-NLC, ZEA-NLC, and B-NLC can be considered stable. Compared to available literature data, obtained particles showed slightly more negative zeta potential, closer to  $-30$  mV (29, 30, 34) and that can be considered beneficial for achieving long-term storage stability.

The *EE* is considered the major factor to be considered when assessing the applicability of NLCs as carriers of bioactive molecules. The *EE* of ASTA-NLC was  $58.0 \pm 6.9\%$ , which is similar to the value reported by Huang and coworkers (31) and lower than reported previously by Tamjidi and coworkers (29) and Rodriguez-Ruiz and coworkers (30). On the other hand, the *EE* of ZEA-NLC was significantly higher compared to the ASTA-NLC. Interestingly, despite similar physicochemical characteristics, data revealed statistically significant differences in *EE* of ASTA and ZEA ( $58 \pm 7\%$  vs.  $76 \pm 2\%$ ). Since *EE* is directly influenced by the solubility of the analyte in the lipid blend, the difference in *EE* of ASTA and ZEA is probably due to the difference in their  $\log p$  values ( $\log p$  of ASTA is 8.163 while  $\log p$  of ZEA is 14.950) indicating higher liposolubility of ZEA (39).

ASTA-NLC, ZEA-NLC, and B-NLC were shown to be stable during a 21-day-storage period in the dark both at room temperature and at  $4^\circ\text{C}$ . That can be considered among

crucial characteristics for their potential utilization in food or pharmaceutical applications. A similar investigation, also reported good stability of ASTA-NLC over a 30-day period (30) while other authors reported notable changes in physicochemical parameters of ASTA-solid lipid nanoparticles and ASTA-loaded liposomes (7, 8). This indicates a certain advantage of NLC as a lipid-based delivery system in the case of ASTA compared to other nanoparticle-based delivery systems.

Investigation of GI stability showed that both ASTA-NLC and ZEA-NLC did not change their effective diameter and *PDI* under gastric conditions. On the other hand, a statistically significant increase of both effective diameter and *PDI* of ASTA-NLC and ZEA-NLC was observed during the intestinal phase of digestion. Other literature data on the GI stability of ASTA-NLC are scarce – good stability of ASTA-NLC in gastric conditions has been observed by Mao and coworkers (40) suggesting NLC suitability as the stable carrier for ASTA. To our knowledge, the GI stability of ZEA-NLC has not been investigated to date. Our results showed a 61 nm increase in ASTA-NLC effective diameter and a 106 nm increase in ZEA-NLC effective diameter under intestinal conditions. The polydispersity of ASTA-NLC increased from 0.128 in water to 0.262 in FaSSIF while for ZEA-NLC increased from 0.122 in water to 0.264 in FaSSIF indicating less uniformed size distribution of particles under GI conditions. Similar phenomena were also reported and explained by the impact of anionic components such as free fatty acids, phospholipids, and bile salts present in the reaction mixture (31, 40).

To our knowledge, this is the first study investigating the impact of NLC formulation on the intestinal permeability of ASTA and ZEA. For this purpose, Caco-2 and Caco-2/HT29 cell models were used and obtained results were compared accordingly (24).

Biocompatibility evaluation showed the low toxicity of lipid nanocarriers loaded with ASTA/ZEA that was already noted by others (17, 41) confirming the advantages of utilizing GRAS excipients in the delivery system formulations. Results showed that both ASTA and ZEA intestinal absorption significantly increased when they were applied in the form of NLCs. The intestinal permeability of ASTA-NLC increased by 3-fold and that of ZEA-NLC by 2-fold with respect to the free form. This is consistent with available literature data since the advantages of lipid-containing delivery systems (nanoemulsions and liposomes) for improving ASTA permeability were already proven by several authors in Caco-2 cells (11, 12, 42). Also, the obtained results are in accordance with the conclusions of the small number of *in vivo* studies that strongly suggest that the bioavailability of ASTA can be significantly improved when taken with meal/lipids (18, 19). With proven good physicochemical properties, satisfactory stability, and positive impacts on intestinal permeability, obtained NLCs could be excellent candidates for delivery systems of ASTA/ZEA as nutraceuticals or functional food ingredients. This study makes a promising foundation for future research on ASTA/ZEA-loaded NLCs and their biointeractions.

ASTA and ZEA intestinal permeability is positively affected by mucus while the effect was lower and inconsistent when they were applied in the form of NLC (positively affecting only the permeability of ASTA-NLC). The available literature data on this subject are scarce and contradictory since some authors concluded that the mucus presence relates to lower permeability of hydrophobic bioactive compounds while others showed improved permeability of lipid-based delivery through the mucus barrier (which is consistent with our results). Li and coworkers (20) reported that the mucus layer covering cocultures was associated with the lower recoveries of beta carotene. On the other hand, Cai and coworkers

(21) recently reported that hydrophobic cinnamaldehyde in self-emulsifying drug delivery systems (SEDDS) exhibited good release and superior mucus permeability.

It is also important to note that in this study no difference was observed in the intestinal absorption of ASTA and ZEA when examined on the Caco-2 cell model but the difference in intestinal absorption was clear on the Caco-2/HT29 co-culture cell model. Namely, in the mucus model, intestinal absorption of ZEA was significantly higher compared to ASTA. On the other hand, ASTA-NLC intestinal absorption was significantly higher compared to ZEA-NLC, in both models. Our results confirm that mucus should be considered in *in vitro* permeability studies. Also, it has been demonstrated that even minor differences in the physicochemical properties of molecules may have a significant impact on interaction with mucus and that the delivery systems strongly affect their interaction and penetration through the intestinal mucus layer.

## CONCLUSIONS

ASTA-NLC and ZEA-NLC showed satisfactory physicochemical properties in terms of effective diameter, polydispersity, and zeta potential which are considered prerequisites for prolonged stability of drug/nutraceutical delivery systems. NLCs were shown to be stable during 21-day-storage periods in the dark at room temperature or at 4 °C. GI stability study confirmed that NLCs do not change their characteristics in gastric conditions, but they increase in size and partially lose their homogeneity in intestinal conditions. Both ASTA and ZEA intestinal permeability were significantly improved when applied in the form of NLC. Investigation on the impact of mucus on ASTA/ZEA permeability revealed significant (mainly positive) influence that varied depending on the type of the investigated substance/delivery system, indicating that mucus should be taken into account in permeability studies of liposoluble compounds. This study provided valuable knowledge on the possibilities of incorporation of ASTA and ZEA into NLCs for improving functionality and enhancing potential applications in the food and pharmaceutical industry.

*Conflict of interest.* – Authors declare no conflict of interest.

*Funding.* – This work was financially supported by UNGAP COST Action CA16205 (European Cooperation in Science and Technology). The authors also thank the FarmInova project [grant number KK.01.1.1.02.0021] funded by the European Regional Development Fund and FCT/MEC [CEEC-INST/00007/2021 and SFRH/BD/147038/2019) financed by Portuguese national funds.

*Authors contributions.* – experimental work, K.R.; interpretations of results, K.R.; original draft preparation, K.R.; methodology, A.I.B.; review and editing, S.R.; conceptualization, M.M.; design of experiments, S.A.C.L.; review and editing, S.A.C.L. and D.V.Č.; formal analysis, D.V.Č.; funding acquisition, D.V.Č. All authors have read and agreed to the published version of the manuscript.

## REFERENCES

1. E. Yamashita, Astaxanthin as a medical food, *Funct. Foods Heal. Dis.* 3(7) (2013) 254–258; <https://doi.org/10.31989/FFHD.V3I7.49>
2. S. Weintraub, T. Shpigel, L. G. Harris, R. Schuster, E. C. Lewis and D. Y. Lewitus, Astaxanthin-based polymers as new antimicrobial compounds, *Polym. Chem.* 8(29) (2017) 4182–4189; <https://doi.org/10.1039/C7PY00663B>

3. J. Zhang, S. Zhang, J. Bi, J. Gu, Y. Deng and C. Liu, Astaxanthin pretreatment attenuates acetaminophen-induced liver injury in mice, *Int. Immunopharmacol.* **45** (2017) 26–33; <https://doi.org/10.1016/j.intimp.2017.01.028>
4. A. G. Murillo, S. Hu and M. L. Fernandez, Zeaxanthin: Metabolism, properties, and antioxidant protection of eyes, Heart, Liver, and Skin, *Antioxidants* **8** (2019) Article ID 390 (18 pages); <https://doi.org/10.3390/ANTIOX8090390>
5. R. F. S. Gonçalves, J. T. Martins, C. M. M. Duarte, A. A. Vicente and A. C. Pinheiro, Advances in nutraceutical delivery systems: From formulation design for bioavailability enhancement to efficacy and safety evaluation, *Trends Food Sci. Technol.* **78** (2018) 270–291; <https://doi.org/10.1016/j.TIFS.2018.06.011>
6. A. A. Martínez-Delgado, S. Khandual and S. J. Villanueva-Rodríguez, Chemical stability of astaxanthin integrated into a food matrix: Effects of food processing and methods for preservation, *Food Chem.* **225** (2017) 23–30; <https://doi.org/10.1016/j.FOODCHEM.2016.11.092>
7. L. Pan, S. Zhang, K. Gu and N. Zhang, Preparation Of astaxanthin-loaded liposomes: Characterization, storage stability and antioxidant activity, *CYTA - J. Food* **16**(1) (2018) 607–618; <https://doi.org/10.1080/19476337.2018.1437080>
8. M. Li, M. R. Zahi, Q. Yuan, F. Tian and H. Liang, Preparation and stability of astaxanthin solid lipid nanoparticles based on stearic acid, *Eur. J. Lipid Sci. Technol.* **118**(4) (2016) 592–602; <https://doi.org/10.1002/ejlt.201400650>
9. N. Kanojia, N. Sharma, N. Gupta and S. Singh, Applications of nanostructured lipid carriers: Recent advancements and patent review, *Biointerface Res. Appl. Chem.* **12**(1) (2022) 638–652; <https://doi.org/10.33263/BRIAC121.638652>
10. N. Dhiman, R. Awasthi, B. Sharma, H. Kharkwal and G. T. Kulkarni, Lipid Nanoparticles as Carriers for Bioactive Delivery, *Front. Chem.* **9** (2021) Article ID 580118 (19 pages); <https://doi.org/10.3389/fchem.2021.580118>
11. X. Shen, T. Fang, J. Zheng and M. Guo, Physicochemical properties and cellular uptake of astaxanthin-loaded emulsions, *Molecules* **24** (2019) Article ID 727 (12 pages); <https://doi.org/10.3390/molecules24040727>
12. C. R. Domínguez-Hernández, M. A. García-Alvarado, H. S. García-Galindo, M. A. Salgado-Cervantes and C. I. Beristáin, Stability, antioxidant activity and bioavailability of nano-emulsified astaxanthin, *Rev. Mex. Ing. Quim.* **15** (2016) 457–468; <https://doi.org/10.24275/RMIQ/ALIM1143>
13. C. H. Peng, C. H. Chang, R. Y. Peng and C. C. Chyau, Improved membrane transport of astaxanthin by liposomal encapsulation, *Eur. J. Pharm. Biopharm.* **75**(2) (2010) 154–161; <https://doi.org/10.1016/j.EJPB.2010.03.004>
14. A. Sangsuriyawong, M. Limpawattana, D. Siriwan and W. Klaypradit, Properties and bioavailability assessment of shrimp astaxanthin loaded liposomes, *Food Sci. Biotechnol.* **28**(2) (2019) 529–537; <https://doi.org/10.1007/s10068-018-0495-x>
15. V. Kakkar and I. P. Kaur, Evaluating potential of curcumin loaded solid lipid nanoparticles in aluminium induced behavioural, biochemical and histopathological alterations in mice brain, *Food Chem. Toxicol.* **49**(11) (2011) 2906–2913; <https://doi.org/10.1016/j.FCT.2011.08.006>
16. H. Yu and Q. Huang, Improving the oral bioavailability of curcumin using novel organogel-based nanoemulsions, *J. Agric. Food Chem.* **60**(21) (2012) 5373–5379; <https://doi.org/10.1021/jf300609p>
17. A. Teo, S. J. Lee, K. K. T. Goh and F. M. Wolber, Kinetic stability and cellular uptake of lutein in WPI-stabilised nanoemulsions and emulsions prepared by emulsification and solvent evaporation method, *Food Chem.* **221** (2017) 1269–1276; <https://doi.org/10.1016/j.foodchem.2016.11.030>
18. Y. Okada, M. Ishikura and T. Maoka, Bioavailability of astaxanthin in *Haematococcus* algal extract: the effects of timing of diet and smoking habits, *Biosci. Biotechnol. Biochem.* **73**(9) (2009) 1928–1932; <https://doi.org/10.1271/BBB.90078>

19. J. M. Odeberg, Å. Lignell, A. Pettersson and P. Höglund, Oral bioavailability of the antioxidant astaxanthin in humans is enhanced by incorporation of lipid based formulations, *Eur. J. Pharm. Sci.* **19**(4) (2003) 299–304; [https://doi.org/10.1016/S0928-0987\(03\)00135-0](https://doi.org/10.1016/S0928-0987(03)00135-0)
20. Y. Li, E. Arranz, A. Guri and M. Corredig, Mucus interactions with liposomes encapsulating bioactives: Interfacial tensiometry and cellular uptake on Caco-2 and cocultures of Caco-2/HT29-MTX, *Food Res. Int.* **92** (2017) 128–137; <https://doi.org/10.1016/j.foodres.2016.12.010>
21. Y. Cai, L. Liu, M. Xia, C. Tian, W. Wu, B. Dong and X. Chu, SEDDS facilitate cinnamaldehyde crossing the mucus barrier: The perspective of mucus and Caco-2/HT29 co-culture models, *Int. J. Pharm.* **614** (2022) Article ID 121461; <https://doi.org/10.1016/j.IJPHARM.2022.121461>
22. D. Resende, S. A. Costa Lima and S. Reis, Nanoencapsulation approaches for oral delivery of vitamin A, *Colloids Surfaces B Biointerfaces* **193** (2020) Article ID 111121; <https://doi.org/10.1016/j.colsurfb.2020.111121>
23. S. Klein, The use of biorelevant dissolution media to forecast the in vivo performance of a drug, *AAPS J.* **12** (2010) 397–406; <https://doi.org/10.1208/S12248-010-9203-3>
24. I. Hubatsch, E. G. E. Ragnarsson and P. Artursson, Determination of drug permeability and prediction of drug absorption in Caco-2 monolayers, *Nat. Protoc.* **2** (2007) 2111–2119; <https://doi.org/10.1038/nprot.2007.303>
25. B. Press, Optimization of the Caco-2 permeability assay to screen drug compounds for intestinal absorption and efflux, *Methods Mol. Biol.* **763** (2011) 139–154; [https://doi.org/10.1007/978-1-61779-191-8\\_9](https://doi.org/10.1007/978-1-61779-191-8_9)
26. N. Ghalandarlaki, A. M. Alizadeh and S. Ashkani-Esfahani, Nanotechnology-applied curcumin for different diseases therapy, *Biomed. Res. Int.* **2014** (2014) Article ID 394264 (23 pages); <https://doi.org/10.1155/2014/394264>
27. D. J. McClements, F. Li and H. Xiao, The nutraceutical bioavailability classification scheme: Classifying nutraceuticals according to factors limiting their oral bioavailability, *Annu. Rev. Food Sci. Technol.* **6** (2015) 299–327; <https://doi.org/10.1146/annurev-food-032814-014043>
28. R. A. Cone, Barrier properties of mucus, *Adv. Drug Deliv. Rev.* **61**(2) (2009) 75–85; <https://doi.org/10.1016/j.addr.2008.09.008>
29. F. Tamjidi, M. Shahedi, J. Varshosaz and A. Nasirpour, Stability of astaxanthin-loaded nanostructured lipid carriers as affected by pH, ionic strength, heat treatment, simulated gastric juice and freeze-thawing, *J. Food Sci. Technol.* **54** (2017) 3132–3141; <https://doi.org/10.1007/s13197-017-2749-7>
30. V. Rodriguez-Ruiz, J. Á. Salatti-Dorado, A. Barzegari, A. Nicolas-Boluda, A. Houaoui, C. Caballo, N. Caballero-Casero, D. Sicilia, J. B. Venegas, E. Pauthe, Y. Omid, D. Letourneur, S. Rubio, V. Gueguen and G. Pavon-Djavid, Astaxanthin-loaded nanostructured lipid carriers for preservation of antioxidant activity, *Molecules* **23**(10) (2018) Article ID 2601 (12 pages); <https://doi.org/10.3390/molecules23102601>
31. J. Huang, W. Xie, L. Liu, Y. Song, F. Pan, H. Bai, T. Pan, Y. Lv, J. Chen, J. Shi and X. Hu, Nanostructured lipid carriers in alginate microgels for the delivery of astaxanthin, *Eur. J. Lipid Sci. Technol.* **123**(2) (2021) Article ID 2000191; <https://doi.org/10.1002/ejlt.202000191>
32. R. Osanlou, M. E. Emtiazjoo, A. Banaei M. Ali Hesarinejad and F. Ashrafi, Evaluation of in vitro release of zeaxanthin-containing nanocarriers, *J. Biol. Stud.* **5** (2022) 512–521; Retrieved from <https://onlinejbs.com/index.php/jbs/article/view/7067>
33. T. Mudalige, H. Qu, D. Van Haute, S. M. Ansar, A. Paredes and T. Ingle, *Characterization of Nanomaterials: Tools and Challenges*, *Nanomater. Food Appl.* Elsevier Inc Amsterdam 2019, pp. 313–353; <https://doi.org/10.1016/B978-0-12-814130-4.00011-7>
34. R. Osanlou, M. Emtiazjoo, A. Banaei, M. A. Hesarinejad and F. Ashrafi, Preparation of solid lipid nanoparticles and nanostructured lipid carriers containing zeaxanthin and evaluation of physi-

- cochemical properties, *Colloids Surfaces A Physicochem. Eng. Asp.* **641** (2022) Article ID 128588; <https://doi.org/10.1016/j.colsurfa.2022.128588>
35. L. A. S. Bahari and H. Hamishehkar, The impact of variables on particle size of solid lipid nanoparticles and nanostructured lipid carriers: A comparative literature review, *Adv. Pharm. Bull.* **6**(2) (2016) 143–151; <https://doi.org/10.15171/APB.2016.021>
  36. D. J. McClements and J. Rao, Food-grade nanoemulsions: formulation, fabrication, properties, performance, biological fate, and potential toxicity, *Crit. Rev. Food Sci. Nutr.* **51**(4) (2011) 285–330; <https://doi.org/10.1080/10408398.2011.559558>
  37. K. Mitri, R. Shegokar, S. Gohla, C. Anselmi and R. H. Müller, Lipid nanocarriers for dermal delivery of lutein: Preparation, characterization, stability and performance, *Int. J. Pharm.* **414**(1–2) (2011) 267–275; <https://doi.org/10.1016/j.ijpharm.2011.05.008>
  38. S. A. Wissing and R. H. Müller, Solid lipid nanoparticles as carrier for sunscreens: In vitro release and in vivo skin penetration, *J. Control. Release* **81**(3) (2002) 225–233; [https://doi.org/10.1016/S0168-3659\(02\)00056-1](https://doi.org/10.1016/S0168-3659(02)00056-1)
  39. D. S. Wishart, A. C. Guo, E. Oler, F. Wang, A. Anjum, H. Peters, R. Dizon, Z. Sayeeda, S. Tian, B. L. Lee, M. Berjanskii, R. Mah, M. Yamamoto, J. Jovel, C. Torres-Calzada, M. Hiebert-Giesbrecht, V. W. Lui, D. Varshavi, D. Allen, D. Arndt, N. Khetarpal, A. Sivakumaran, K. Harford, S. Sanford, K. Yee, X. Cao, Z. Budinski, J. Liigand, L. Zhang, J. Zheng, R. Mandal, N. Karu, M. Dambrova, H. B. Schiöth, R. Greiner and V. Gautam,, HMDB 5.0: the Human Metabolome Database for 2022, *Nucleic Acids Res.* **50**(D1) (2022) D622–D631; <https://doi.org/10.1093/NAR/GKAB1062>
  40. X. Mao, Y. Tian, R. Sun, Q. Wang, J. Huang and Q. Xia, Stability study and in vitro evaluation of astaxanthin nanostructured lipid carriers in food industry, *Integr. Ferroelectr.* **200**(1) (2019) 208–216; <https://doi.org/10.1080/10584587.2019.1592626>
  41. S. Doktorovová, A. B. Kovačević, M. L. Garcia and E. B. Souto, Preclinical safety of solid lipid nanoparticles and nanostructured lipid carriers: Current evidence from in vitro and in vivo evaluation, *Eur. J. Pharm. Biopharm.* **108** (2016) 235–252; <https://doi.org/10.1016/j.ejpb.2016.08.001>
  42. K. Karim, A. Mandal, N. Biswas, A. Guha, S. Chatterjee, M. Behera and K. Kuotsu, Niosome: A future of targeted drug delivery systems, *J. Adv. Pharm. Technol. Res.* **1**(4) (2010) 374–380; <https://doi.org/10.4103/0110-5558.76435>